9072 *J. Phys. Chem. A* **1999,** *103,* 9072−9079

Electron Affinity, Gas-Phase Acidity, Bond Dissociation Energy, and Negative Ion States of Nitromethane

Edward C. M. Chen* and Natalie Welk
University of Houston Clear Lake, 2700 Bay Area Blvd., Houston, Texas 77058

Edward S. Chen
Center for Research in Parallel Computation, Rice University, Houston, Texas 77005

W. E. Wentworth
Department of Chemistry, University of Houston, Houston, Texas 77002

Received: February 11, 1999; In Final Form: August 16, 1999

Published electron capture detector (ECD) data for nitromethane and α-nitrotoluene were analyzed using the nonlinear least-squares procedure. From this, the adiabatic electron affinities are 0.50 ± 0.02 and 0.65 ± 0.1 eV and the CN bond dissociation energies are 2.67 ± 0.1 and 2.0 ± 0.1 eV, respectively. Negative ion Morse potentials consolidate diverse data for nitromethane in both the CN and CH dimensions. Curves for α-nitrotoluene were predicted by analogy to the nitromethane curves. Semiempirical multiconfiguration configuration interaction (AM1-MCCI) calculations support the above ECD values. For nitromethane, the calculated values are $D(\mathrm{CH}) = 4.42$ eV, $\mathrm{EA(CH_2NO_2)} = 2.45$ eV, and gas-phase acidity (GPA) = 15.4 eV. These agree with experimental literature values. Comparable predicted values for α-nitrotoluene are $D(\mathrm{CH}) = 3.8$ eV, $\mathrm{EA(C_7H_6NO_2)} = 2.4$ eV, and GPA = 15.0 eV.

Introduction

The formation and destruction of negative ions in nitromethane CH_3NO_2 has been studied by many different techniques.[1−19] However, there are uncertainties in important properties such as the adiabatic electron affinity (AEA) and the bond dissociation energy, D(CN). The adiabatic electron affinity is the energy difference between the anion and the neutral in their most stable states. The vertical electron affinity (VEA) is the energy difference in the geometry of the neutral. The (DBEA) is a specific type of VEA for molecules with large dipole moments. By convention, EAs are positive for exothermic reactions. The photodetachment or vertical detachment energy (VDE) is the energy difference in the geometry of the anion. The absorbance maximum (E_{abs}) is the peak energy in the absorption spectra of the ground-state anion. The gas-phase acidity (GPA) of XH is $\mathrm{IP(H)} + D(\mathrm{XH}) - \mathrm{EA(X)}$ so that $D(\mathrm{XH}) - \mathrm{EA(X)} = \mathrm{IP(H)} - \mathrm{GPA}$, where IP(H) is the ionization potential of the H atom.

The reported adiabatic electron affinities for nitromethane range from 0.26 ± 0.08 to 0.5 ± 0.1 eV.[1−3,5,7,9−14] An average value of 0.45 ± 0.05 eV was obtained from two determinations, one in 1969 and one in 1971. Both used electron capture (ECD) data, but neither was published in the open literature until 1983.[1−3] Several values, each with an error of 0.2 eV, were determined using the alkali metal beam technique in the late 1970s. The average of three values is 0.44 ± 0.12 eV.[5,7,9] In 1988, a value of 0.5 ± 0.1 eV was obtained from thermal charge transfer experiments.[8] In 1996, the most recent value, 0.26 ± 0.08 eV, was reported. The adiabatic electron affinity was assigned to the first discernible peak in the photoelectron spectrum. No dipole bound state was identified. It was stated, “We estimate that $CH_3NO_2^-$ has about 190 states with energy less than 0.26 eV. ”[10] The existence of a dipole bound state was predicted by theoretical calculations.[11]

The first purpose of this paper is to present the results of a nonlinear least-squares analysis of two sets of ECD data collected for nitromethane to obtain 0.50 ± 0.02 eV for the AEA and $D(\mathrm{CN}) - \mathrm{AEA(NO_2)} = 0.31 \pm 0.05$ eV. From this experimental value and the literature value for the $\mathrm{EA(NO_2)} = 2.36$ eV, the carbon nitrogen bond dissociation energy is 2.67 ± 0.1 eV compared to the literature value, 2.64 ± 0.1 eV.[15] A similar least-squares analysis is applied to unpublished ECD data for α-nitrotoluene, $C_7H_7NO_2$.[2]

The second purpose of this paper is to present multiple “two-dimensional” Morse potential energy curves for anions of CH_3NO_2 constructed in the CN and CH dimensions from experimental data, including the absorption and emission spectrum of the nitromethane anion, the gas-phase acidity of nitromethane, and the electron affinity of the CH_2NO_2 radical.[16−19] Multiple states have been observed for molecules with large adiabatic electron affinities.[20] The procedure of consolidating diverse data to obtain Morse potentials has been described for the diatomic halogen anions, rare gas cations, the negative ion states of SF_6, and the anions of chloroethylenes.[13,21−23]

The use of two-dimensional Morse potentials for dissociative electron attachment reactions and parent negative ion formation in polyatomic molecules is only an approximation to a multidimensional surface. In the past, such curves would be used cautiously. However, recently a theory of vibrational relaxation in resonant collisions of electrons with large molecules was proposed. It was concluded that “vibrational relaxation results from the coupling of a few active modes which are strongly coupled to the electronic degrees of freedom and therefore are coherently excited during the formation of the complex.”[24] The

10.1021/jp990530l CCC: $18.00

use of the CH and CN reaction coordinates is thus an appropriate way to visualize the electron molecule interaction.

Morse potential energy curves for a dipole bound state and a valence state for CH_3NO_2 were proposed in 1978. The valence state had a CN distance larger than for the neutral and dissociated to CH_3 plus $NO_2(-)$. The dipole bound state had the same CN distance as the neutral, 1.47 Å, but did not have a definite dissociation limit.[5,7] In 1991, two bound excited states (D and E) were proposed dissociating to CH_3 plus $NO_2*(-)$ and to CH_3 plus $NO_2**(-)$.[9] These curves have been used to support the postulate that absorption and emission spectra observed in a shock tube experiment with liquid nitromethane were due to the anion.[16]

Another objective is to use the AM1 semiempirical multiconfiguration configuration interaction (AM1-MCCI) procedure to calculate EA(CH_3NO_2), EA($C_7H_7NO_2$), *D*(CN), *D*(CH), and EA(CH_2NO_2), to support the experimental results. A descriptive acronym for the procedure is the use of Configuration Interaction or Unrestricted Orbitals to Relate Experimental Electron Affinities to Self-Consistent Field Values by Estimating Electron Correlation (CURES EC). The objective is to minimize σ(EA) = |{EA(CURES EC) − EA(experimental)}|. To date, CURES EC has been successfully applied [σ(EA) < 0.1 eV] to 300+ molecules and radicals.[25−29] A newly developed quantum mechanical computer simulation will be used to verify adiabatic electron affinities. This is designated READS TCT for the estimation of Relative Electron Affinities by Dimolecular Simulation of Thermal Charge Transfer experiments. The acronym clearly describes the purpose of the simulation.

Kinetic Model of the ECD

The kinetic model of the ECD has been described previously.[1−3,12,25,30−31] It also applies to thermal negative ion mass spectrometry, NIMS.[30] The ECD reactions are

$$AB + e^- \underset{k_{-1}}{\overset{k_1}{\Leftrightarrow}} AB(-) \xrightarrow{k_2} A + B(-)$$

$$e^- + P^+ \xrightarrow{k'_D} \text{neutrals}$$

$$AB(-) + P^+ \xrightarrow{k'_N} \text{neutrals}$$

Assuming constant positive ion concentrations, k'_D and k'_N can be replaced with pseudo unimolecular rate constants k_D and k_N.

The experiment consists of measuring the molar response of the ECD or NIMS as a function of temperature. The NIMS data are the abundance of the specific ions. The molar response is simply the integrated count per mole of a sample molecule, AB. In the ECD, the data are I_{e-} , the electron current in the presence, and I_b, the electron current in the absence of the capturing species. At steady state and low capture

$$\{I_b - I_{e-}\}/I_{e-} = K[AB]/2 \qquad (1)$$

In general, *K* can be related to the rate constants for two states as[25]

$$K = \left[\frac{k_1(k_N + k_2)}{2(k_D)(k_{-1} + k_N + k_2)}\right](gs) + \left[\frac{k_1(k_N + k_2)}{2(k_D)(k_{-1} + k_N + k_2)}\right](xs) \qquad (2)$$

where gs refers to the ground state and xs refers to an excited state. In the case of the nitro compounds, only one state is involved.

Four temperature regions have been defined based on relative values of the rate constants. From low to high temperatures, they are the β region, where ($k_N \gg k_{-1} + k_2$) and $K = k_1/2k_D$; the α region, where ($k_{-1} \gg k_N + k_2$) and $K = [k_N/2k_D][k_1/k_{-1}]$; the γ region, where ($k_2 \gg k_N$) and ($k_{-1} \gg k_2$), and $K = [k_2/2k_D][k_1/k_{-1}]$; and the δ region, where ($k_2 \gg k_{-1} + k_N$) and $K = k_1/2k_D$. In the α region, the absolute electron affinity is obtained.

From eq 2 and the kinetic expressions given below an equation for least-squares analysis can be obtained:

$$k_N = A_N = \text{constant}; \quad k_D = A_D = \text{constant}$$

$$k_1 = A_1 T^{-1/2} \exp(-E_1/RT)$$

$$k_{-1} = A_{-1} T \exp(-E_{-1}/RT)$$

$$k_2 = A_2 T \exp(-E_2/RT)$$

The number of parameters for the nitrocompounds is six, two each for the three rate constants. The least-squares equation is

$$K = \frac{A_1 T^{-1/2} \exp(-E_1/RT)\{A_N + A_2 T \exp(-E_2/RT)\}}{2A_D[A_N + A_{-1} T \exp(-E_{-1}/RT) + A_2 T \exp(-E_2/RT)]} \qquad (3)$$

These data will exhibit an α and a γ region. The values of A_1 and E_1 are systematically fixed and the other quantities determined. For nitrotoluene, there is only one temperature region. The α and γ regions merge with each other. The absolute electron affinity is obtained from the slope in the α region:

$$K = [k_N/2k_D][k_1/k_{-1}] = [k_N/2k_D][A_1/A_{-1}]T^{-3/2}\{\exp(EA/RT)\} \qquad (4)$$

$$\text{Ln } KT^{3/2} = \text{Ln}(A_N/2A_D) + \text{Ln}(A_1/A_{-1}) + EA/RT \qquad (5)$$

The slope in a plot of Ln $KT^{3/2}$ vs 1000/*T* is EA/*R*. The intercept is Ln($A_N/2A_D$)+ Ln(A_1/A_{-1}). By using the statistical mechanical expression for $k_1/k_{-1} = K_{eq}$ for the reaction of thermal electrons with molecules

$$(A_1/A_{-1}) = [g(A^-)/g(A)]h^3/(2\pi m_e k)^{3/2} \qquad (6)$$

where m_e is the electron mass and *k* and *h* are the Boltzmann and Planck constants. The *g*'s are partition functions, and Ln(A_1/A_{-1}) = 12.43 + Ln($A_N/2A_D$) + Ln([$g(A^-)/g(A)$]). The intercept involves the ratio of ($A_N/2A_D$) so that the concentration of the positive species and the temperature dependence of the intrinsic rate constants will cancel and not affect the value of the slope. A value of $A_N/2A_D$ can be obtained by measuring the ECD temperature dependence of a compound with an accurate AEA and a unit partition function ratio such as acetophenone. From an estimate of Ln($A_N/2A_D$), and an experimental intercept, [$g(A^-)/g(A)$], the partition function ratio, PFR, can be calculated. The observed PFR values range from 1 to 10^{-4}. The ECD and NIMS experiments are the only ones that have been used extensively to measure PFR values.

In the γ region, the slope is approximately equal to (EA − E_2) since $K = [k_2/2k_D][k_1/k_{-1}]$ and

$$\text{Ln } KT^{3/2} = \text{Ln}(T/2A_D) + \text{Ln}(A_2A_1/A_{-1}) + (\text{EA} - E_2)/RT \qquad (7)$$

Since E_2 is greater than EA, there will be a change of the direction of the slope in the transition from the α to the γ region. The experimental quantity, (EA − E_2) is equal to D(CN) − EA(NO_2).

In the β or δ region, $K = k_1/2k_D$ and the ECD data defines A_1 and E_1. Alternatively, if the values of A_1 and E_1 are known accurately, such as for CCl_4, A_D can be obtained from the ECD data. The A_1 for electron attachment is related to $\pi\lambda^2$, where λ is the de Broglie wavelength of the electron which can be calculated from fundamental constants. The maximum value of A_1 is the de Broglie A_1 value, (DeBA). The value for ln(DeBA) is about 35−36.

Quantum Mechanical Calculations

The quantum mechanical calculations are carried out on a Pentium desktop computer with commercial software (HYPERCHEM). The first step in CURES EC is to estimate the EA. This can be an experimental gas-phase value, or one obtained by calibration of half-wave reduction potentials to gas-phase values, or can be an estimate based on substitution and replacement rules. For example, the electron affinities of adenine, guanine, cytosine, uracil, and thymine were first estimated by substitution and replacement rules. Next, they were estimated by measurement of half-wave reduction potentials in aprotic solvents and scaling to absolute electron affinities measured in the gas phase.[32] These have been confirmed by CURES EC calculations.[28,29] These are the only experimental and theoretically verified AEAs of adenine, guanine, cytosine, uracil, and thymine. Recently, dipole bound and valence state anions of the nucleic acids have been observed in the gas phase and the electron impact and electron transmission spectra have been measured.[33−35] On the basis of these data, Morse potentials can be calculated for the negative ion states of these species in the same manner as with nitromethane and α-nitrotoluene. This will be the subject of a future publication.

Once the AEA is estimated, the geometry optimization quantum mechanical calculations are carried out for both the neutral and the negative ion, sometimes by annealing the geometry. Then MCCI is added. The EA is the difference in the electronic energies of the neutral and the negative ion at the global minimum. The CURES EC result is designated as UHF- or RHF(*aann*), where the *aa* refers to the number of filled and unfilled orbitals used in the MCCI for the anion and the *nn* refers to those for the neutral. The UHF and RHF values for closed orbital species are the same. The CURES EC procedure can only improve upon the UHF- or RHF(0000) values since these can be the optimum. These AEA are quantum properties since the *a* and *n* values are integers. In the case of the aromatic hydrocarbons, the MINDO/3(*aa*00) procedure is usually the most appropriate. In the case of the purines and pyrimidines and other molecules containing C, H, O, N, and the halogens, the AM1(*aann*) procedure is the most appropriate. For the nitro compounds the most appropriate is AM1(0033). For C_{60} the MNDO(0033) calculated value of 2.75 eV is in agreement with the experimental AEA (2.666 ± 0.001 eV).[36]

Another method of verifying experimental results is to simulate the thermal charge transfer experiments. The test molecule is merged with anions of species with measured AEA. This then brackets the value for the test species. The quantum mechanical calculation is carried out, and the charge densities on the two molecules are observed. The relative charge density is greater than unity for a molecule with an AEA lower than the test AEA and less than unity for one with an AEA higher than for the test molecule. The radicals formed from nitromethane and α-nitrotoluene by the removal of a hydrogen atom and NO_2 should have about the same AEA, so the ratio should be about unity.

Morse Potential Energy Curves

The Morse potentials for the neutral as referenced to zero energy at infinite separation and the parametrized Morse potential for the anions are given by[21−23]

$$U(\text{RNO}_2) = -2D_e(\text{RNO}_2)\exp(-\beta(r - r_e)) + 2D_e(\text{RNO}_2)\exp(-2\beta(r - r_e)) \qquad (8)$$

$$U(\text{RNO}_2^-) = -2k_AD_e(\text{RNO}_2)\exp(-k_B\beta(r - r_e)) + k_RD_e(\text{RNO}_2)\exp(-2k_B\beta(r - r_e)) - \text{EA}(\text{NO}_2) \qquad (9)$$

where $D_e(\text{RNO}_2)$ represents the bond dissociation energy, r is the internuclear separation, $r_e = r$ at the minimum of $U(\text{RNO}_2)$, and EA(NO_2) is electron affinity of NO_2; $\beta = \nu_e(2\pi^2\mu/D_e[\text{RNO}_2])^{1/2}$ with μ, the reduced mass; k_A, k_B, and k_R are dimensionless constants. For curves dissociating to excited states of NO_2(−), the excitation energy must be added to give the proper limit.

$$D_e(\text{RNO}_2^-) = [k_A^2/k_R]D_e(\text{RNO}_2) \qquad (10)$$

$$r_e(\text{RNO}_2^-) = [\ln(k_R/k_A)]/[k_B\,\beta(\text{RNO}_2)] + r_e(\text{RNO}_2) \qquad (11)$$

$$\nu_e(\text{RNO}_2^-) = [k_Ak_B/k_R^{1/2}]\nu_e(\text{RNO}_2) \qquad (12)$$

$$-\text{VEA} = D_e(\text{RNO}_2)(1 - 2k_A + k_R) - \text{EA}(\text{NO}_2) - (1/2)h\upsilon_e(\text{RNO}_2) \qquad (13)$$

$$D_e(\text{RNO}_2^-) = D_e(\text{RNO}_2) - \text{EA}(\text{NO}_2) + \text{AEA}(\text{RNO}_2) \qquad (14)$$

Values of AEA, VEA, and EA(NO_2) give k_A and k_R using eqs 10, 13, and 14. The mass spectrometric ion distribution gives k_B by reflecting the distribution of the neutral onto the negative ion curves. Any three data points on the negative ion curve, including the standard Morse parameters for the anion, can be used to define the dimensionless parameters. Once the values of k_B, k_A, and k_R are obtained, the Morse parameters of the negative ion curve can be calculated from eqs 10−12 and the Morse parameters for the neutral. Thus the negative ion curve is also a Morse curve.

Results and Discussion

Electron Capture Detector and Quantum Mechanical Calculations

Figure 1 shows ECD data for CCl_4 (β region), O_2 (α and β regions), $C_6H_5COCH_3$, acetophenone (α region), nitromethane (α to γ), and nitrotoluene. The use of data for CCl_4 and acetophenone to determine A_D and ($A_N/2A_D$) has been described previously.[25] The curve for O_2 in Figure 1 was obtained by fitting the data to the general ECD equation for a single state (eq 2). The AEA of O_2 is 0.44 eV, the same as determined by many different methods.[12−14,37] The ECD temperature depen-

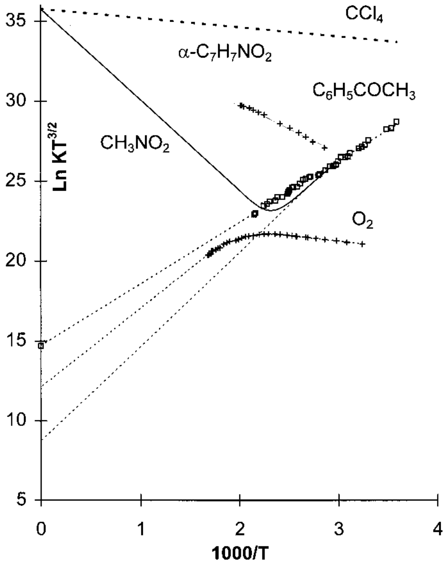

Figure 1. Global plot of electron capture data as Ln($KT^{3/2}$) vs 1000/T. Calculated curves and data for O_2 and acetophenone, and calculated curves for CCl_4 and nitromethane. The O_2 and the α-nitrotoluene data are taken from ref 2 while the use of the acetophenone and CCl_4 data to characterize the detector is discussed in ref 25. The dotted lines with a positive slope are data in the α region, where the adiabatic electron affinity is equal to this slope times R, the gas constant.

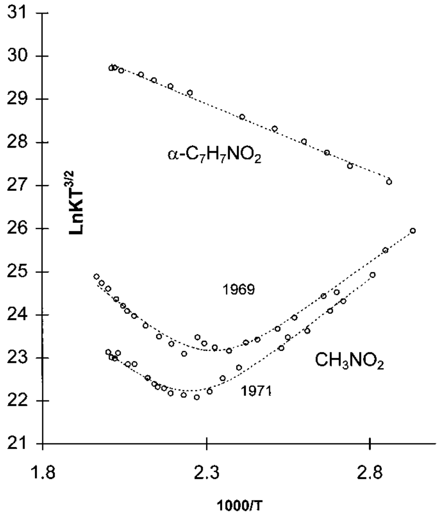

Figure 2. Electron capture data as Ln($KT^{3/2}$) vs 1000/T for nitromethane and α-nitrotoluene originally obtained in 1969 and 1971, refs 1 and 2.

dence of O_2 could have been calculated from literature data and the A_D and A_N values. This is a global plot and illustrates the different types of temperature dependence that have been observed in the ECD. The limiting value of the intercept is determined from the de Broglie A value. The slopes in the α region are proportional to the adiabatic electron affinity of the molecule.

In Figure 2 the ECD data for nitromethane and nitrotoluene are presented on a larger scale. The curves have been obtained from eq 3 with the least-squares parameters shown in Table 1. The CN bond dissociation energy is 2.67 ± 0.1 eV and the AEA 0.50 ± 0.02 eV for nitromethane. The A_1 values were set to the de Broglie A value in agreement with the experimental alkali metal beam results.[7] The activation energy was adjusted manually to give the minimum in the sum of the squares of the residuals. Then the other values of the parameters were obtained by minimizing the weighted sum of the squares of the residuals in an automatic procedure programmed using Excel. The value of the partition function ratio is about 7×10^{-3}. The values of the parameters for nitromethane are consistent from the two experiments within the errors.

TABLE 1: Electron Capture Detector Parameters

	nitromethane		
parameters	1969 data	1971 data	α-nitrotoluene
Ln(A_1)	(36.33)	(36.31)	(36.25)
E_1 (eV)	0.20	0.20	0.23
Ln(A_{-1})	29.44 ± 0.37	29.76 ± 0.43	29.75 ± 0.32
E_{-1} (eV)	0.69 ± 0.02	0.71 ± 0.02	0.89 ± 0.10
AEA (eV)	0.49 ± 0.02	0.51 ± 0.02	0.65 ± 0.10
PFR	7×10^{-3}	9.9×10^{-3}	5×10^{-3}
Ln(A_2)	29.33 ± 0.41	29.50 ± 0.46	29.38 ± 0.42
E_2 (eV)	0.99 ± 0.05	1.02 ± 0.10	0.57 ± 0.10
D(C−N) − EA(X) (eV)	0.32 ± 0.05	0.31 ± 0.10	−0.32 ± 0.10
D(C−N) (eV)	2.68 ± 0.05	2.67 ± 0.10	2.04± 0.10

The parameters A_1, A_{-1}, A_2, and E_1 for nitromethane and their respective errors are included in the least-squares data analysis for α-nitrotoluene to determine the quantities E_{-1} and E_2. The resulting AEA of 0.65 ± 0.1 eV and D(CN) of 2.0 ± 0.1 eV are reasonable. The AEA should be higher than that for nitromethane based on the replacement of a hydrogen atom with a phenyl group. The D(CN) for α-nitrotoluene is 0.65 eV lower than that for nitromethane in agreement with the average difference in the CX bond energies in CH_3X and C_7H_7 X.[15]

The CURES EC calculations using AM1-MCCI (RHF(0033)) of the EA (CH_3NO_2), EA($C_7H_7NO_2$), D(CN), D(CH), and EA(CH_2NO_2) agree with the experimental results within the error. There is a significant change in the geometry of the anion of nitromethane. Also calculated are D(CH) = 4.42 eV, EA(CH_2NO_2) = 2.45 eV, and gas-phase acidity = 15.4 eV for nitromethane in agreement with experiment.[17−19] Similar predicted values for nitrotoluene are D(CH) = 3.8 eV, EA($C_7H_6NO_2$) = 2.4 eV, and GPA = 15.0 eV.

The simulated charge transfer experiments were carried out for the anions of nitromethane, $C_7H_7NO_2$, CH_2NO_2, and $C_6H_5CHNO_2$. Molecular oxygen, AEA = 0.45 eV, transferred charge to all four of the species. The nitromethane anion transfers charge to $C_7H_7NO_2$, placing the electron affinity of nitromethane between 0.45 and 0.65 eV. $C_7H_7NO_2$ receives charge from benz[*e*]pyrene (AEA = 0.56 eV), and gives charge to planar *c*-C_8H_8 (AEA = 0.73 eV).[27,39] Each of the three species receives charge from the methoxy radical (AEA = 1.6 eV).[13,14] In all the dimolecular simulations involving $C_6H_5CHNO_2$, CH_2NO_2, and NO_2 the charge is equally distributed. Thus the electron affinities of the three nitro radicals are comparable and are greater than 1.6 eV. These results support the experimental values and the "absolute" values calculated using CURES EC.

Morse Potential Energy Curves

Morse potential energy curves for nitromethane and α-nitrotoluene are shown in Figures 3−6. In Table 2 the dimensionless constants and the Morse parameters are given. Figures 7 and 8 illustrate the use of electron impact and photoelectron spectroscopy distributions to define the X and A states of nitromethane. Only these low-lying states are defined by experimental data. Approximations for the bond dissociation energies for the other excited-state anions are used. The curves for α-nitrotoluene are predictions by analogy to those for nitromethane. The curves use the ECD data and theoretically calculated properties.

In Figure 3 are the four potential energy curves for nitromethane which have been suggested in the literature.[5,7,9] The curves have been adjusted to reflect the current "best" thermo-

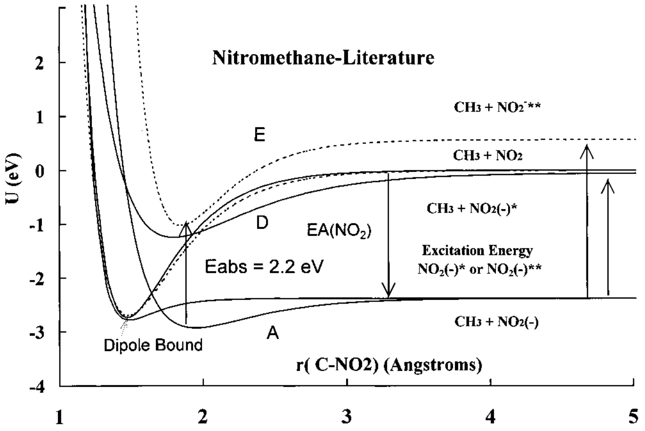

Figure 3. Morse potentials for nitromethane and anions in the C−N dimension as postulated in the literature in refs 5, 7, 9, and 10. Two dipole bound states are indicated dissociating to different limits. The excited states D and E are taken from ref 9.

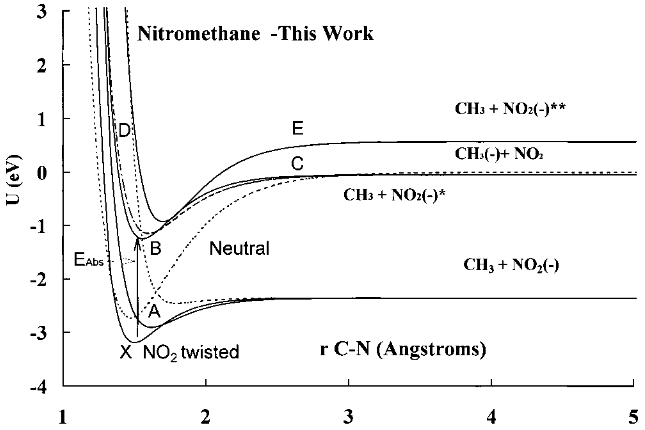

Figure 4. Morse potentials for nitromethane and anions in the C−N dimension. The X and A curves are overdetermined by electron capture (this work), photoelectron spectroscopy (ref 10), electron impact (refs 4 and 6), and absorption spectroscopy (ref 16). There is a change in the geometry for the X state. The E excited state is taken from ref 9.

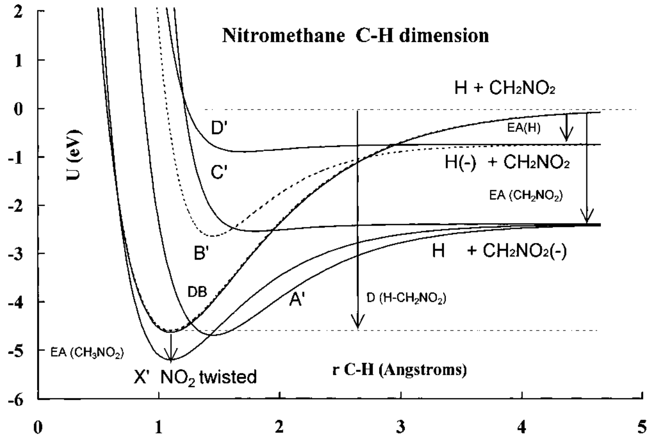

Figure 5. Morse potentials for nitromethane and anions in the C−H dimension. The curves use the values for the adiabatic electron affinity, electron impact data (refs 4 and 6), and estimated bond dissociation energies. There is a change in the geometry for the X state. One dipole bound state is shown.

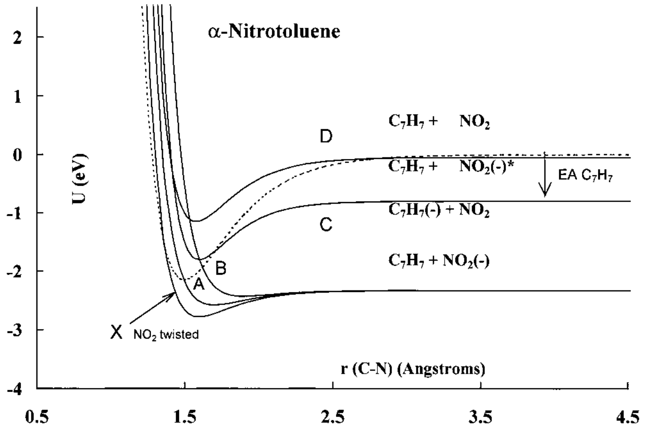

Figure 6. Morse potentials for α-nitrotoluene and anions in the C−N dimension. The curves are calculated by analogy to those for nitromethane.

dynamic data available for the states and the assumption that the state previously assigned as the ground state is an excited state (A). The construction of the D and E curves drawn to excited states of $NO_2(-)$ using alkali metal beam has been described in the literature.[9] Shown in Figure 3 is the transition for the maximum in the absorption spectra at about 2.2 eV. Since the present X state had not been suggested, the transition was assigned to the supposed ground state. The dipole bound state is nearly coincidental with the neutral curve. Two possible dissociation limits for the dipole bound state are shown by analogy to negative ion states of HCl, where more than one dipole-induced limit was suggested.[38]

In Figure 4 the Morse curves based upon the present data are presented. Three new curves X, B, and C are proposed. The dipole bound state curves have not been significantly modified from those shown in Figure 3. The A, D, and E state curves are similar to the earlier ones, but have a smaller CN distance.[11] The X state dissociates to $CH_3 + NO_2(-)$. The NO_2 group is twisted in the ground-state anion relative to the neutral. The A and B dissociate to this same limit, but have a larger CN distance. They are otherwise in the geometry of the neutral. A third state (C) leads to the complementary limit, $CH_3(-)$ plus NO_2. The dissociation limits for CH_3 plus $NO_2{}^*(-)$ and $CH_3(-)$ plus NO_2 are about the same since the adiabatic electron affinity of the methyl radical is small while the excitation energy of $NO_2{}^*(-)$ is about the same as the adiabatic electron affinity of the NO_2 radical.[9,16] These are illustrated in Figures 3−5.

The X curve is defined by the CN distance and frequency, which are the same as for the neutral based on theoretical calculations.[11] The third parameter, the dissociation energy, is determined from the higher adiabatic electron affinity, 0.5 eV.[1−3,7−9] The formation of the ground-state anion requires an activation energy, E_1 , due to the twisting of the nitro group. Once the ground-state curve is defined, the absorption and emission spectra of nitromethane can be used to help define the curves for excited states. In Figure 4, the maximum in the transition is 2.2 eV but the internuclear distance for the excited state is based on the internuclear distance of the X state. The transition is from the X state to the C state. The agreement of the calculated E_{Abs} with the experimental value supports the ground-state curve and the literature assignment of the observed absorption and emission spectrum of the anion of nitromethane.[16] The photoelectron spectrum of the X-state anion will exhibit a sharp peak at 0.5 eV. The experimental spectrum does show a peak at this energy, but it is superimposed on the much larger peak from the A state. The lower intensity could be due to the activation energy for the formation of the ground-state ion.

The A state is defined by the photoelectron spectroscopy distribution, the PES electron affinity of 0.28 eV, and the electron impact distribution and vertical onset for the formation of $NO_2(-)$ at 0.3 eV which peaks at 0.6 eV.[4,6] The calculated

TABLE 2: Morse Parameters and Dimensionless Constants[a]

molecule	k_A	k_B	k_R	D_e (eV)	r_e (pm)	ν (cm^{-1})
nitromethane						
neutral C−N	1.000	1.000	1.000	2.73	147.5	1562
dipole bound	1.002	0.918	1.016	2.7	148	1425
dipole bound	0.158	1.674	0.171	0.40	149	1000
X	0.344	1.627	0.389	0.83	150	1400
A	0.383	1.142	0.730	0.55	166	800
B	0.273	1.255	2.035	0.10	200	375
C	0.656	1.256	0.981	1.20	158	1300
D	0.638	1.211	1.013	1.10	160	1200
E	1.258	1.210	2.886	1.50	170	1400
neutral C−H	1.000	1.000	1.000	4.6	110	3000
dipole bound	0.997	1.002	0.997	4.6	110	3000
X′	0.585	1.308	0.585	2.7	110	3000
A′	0.861	1.181	1.488	2.3	145	2500
B′	0.876	1.519	1.771	2.0	145	3000
C′	0.230	1.849	1.634	0.15	190	1000
D′	0.169	1.883	0.756	0.17	170	1100
nitrotoluene						
neutral C−N	1.000	1.000	1.000	2.15	150	1562
X	0.319	1.328	0.485	0.45	160	950
A	0.267	1.313	0.611	0.25	170	700
B	0.251	1.355	1.355	0.10	190	450
C	0.726	1.407	1.132	1.00	160	1500
D	0.703	1.252	0.964	1.10	158	1400

[a] Only the X and A CN curves for nitromethane are completely defined by experimental data. The others use data where available (see text).

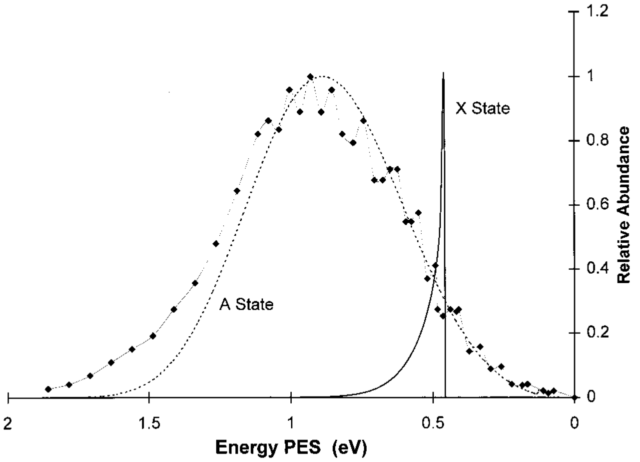

Figure 7. Calculated and experimental photoelectron spectra for the X and A states of the anion of nitromethane in the C−N dimension, Figure 4. The data are taken from ref 10.

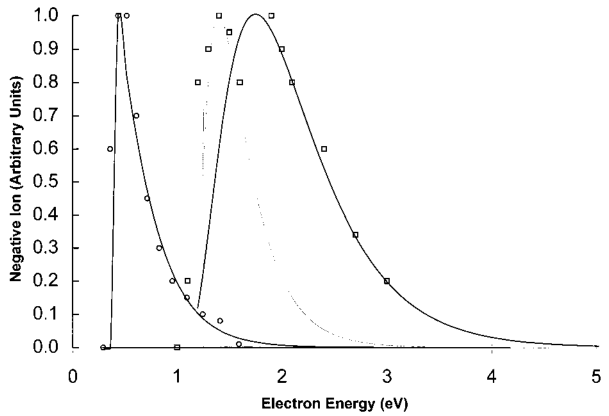

Figure 8. Calculated and experimental electron impact data for the A state of nitromethane in the C−N dimension. The data are taken from ref 4.

and experimental PES distribution for the A state is a broad peak at 0.8 eV as shown in Figure 7. The calculated X-state distribution is shown as a sharp peak at 0.5 eV. The dipole bound state will give a small sharp peak at less than 0.05 eV.[11] The agreement between the calculated and experimental electron impact curves is illustrated in Figure 8. The onset agrees with the ECD value, 0.3 ± 0.05 eV. The A state is defined by more than three points on the curve since ECD, electron impact, and photoelectron spectroscopy data are available. In addition, the values of the Morse parameters for the A state are quite reasonable with a lower bond dissociation energy, a lower frequency, and a larger internuclear distance in the anion than in the neutral, as shown in Table 2.

The B state is defined by a small *D*(CN), a larger CN distance, and a VEA of 4.4 eV from the electron impact data.[4,6] The C and D states are defined by a bond order of about $^1/_2$ and the electron impact ion curves which peak at 1.7 and 2.2 eV. This defines the VEA and the slope of the negative ion curve in the Franck−Condon region. The anion absorption spectra will be similar to the 1.7 eV electron impact peak attributed to the C state, but it will be shifted by the adiabatic electron affinity of nitromethane (i.e., $1.7 + 0.5 = 2.2$ eV). This agrees with the experimental data for the absorption maximum and supports the value of the assumed C-state bond dissociation energy.

Another reaction coordinate for the electron impact of nitromethane is the CH dimension. Five anion curves are shown in Figure 5. In one of the electron impact studies, the CH_2NO_2-(−) ion is observed at 4, 5.8, and 7.5 eV.[6] Two curves are drawn to each dissociation limit, one with a bond order of about $^1/_2$ and the other closer to a dissociative curve. This corresponds to similar curves for the anions of diatomic molecules. These curves are more speculative since less data are available. The ground-state curve is calculated in the same manner as for the C−N dimension and reflects the higher electron affinity of 0.5 eV. A single dipole bound state is illustrated.

In Figure 6 the predicted Morse potentials for α-nitrotoluene are shown. The similarity to those for nitromethane is apparent. One major difference is that dissociative thermal electron attachment is exothermic while that for nitromethane is endothermic. Another major difference is that the electron affinity of the benzyl radical is larger than that for the methyl radical so that the C and D states are more clearly resolved. This supports the postulate of a C state for nitromethane. There are no data to our knowledge to test these curves.

The values for the dimensionless constants and the Morse parameters for the potentials shown in Figures 3−6 are given in Table 2 and are in the nominal ranges. The values for k_B are larger than 1 but not as large as 2 for many of the curves. The values of k_A are generally less than 1, indicating a smaller attraction. The k_R repulsive terms are in the range of 0.2−2, indicating both a decrease and an increase in the repulsion in the anion. For the dipole bound states, the values of k_A and k_R are about the same.

Summary

The nonlinear least-squares analysis of the ECD data for nitromethane and α-nitrotoluene give the adiabatic electron affinities and CN bond dissociation energies. The accuracy and precision of the values for nitromethane are improved. The D(CN) value agrees with the literature value. The ECD adiabatic electron affinity supports the higher values obtained using alkalai metal beam and thermal charge transfer procedures. The values for nitrotoluene are new and unique. The thermodynamic properties obtained from the ECD data are supported by semiempirical calculations of absolute quantities and the determination of relative degrees of charge transfer in a new simulation of thermal charge transfer experiments. Three new states for nitromethane are identified: the ground-state X curve, a near repulsive B state, and a bound C state dissociating to the methyl anion and the NO_2 radical. Morse potential energy curves for six negative ion states of nitromethane in the C−N dimension have been calculated from experimental data including the above ECD, photoelectron spectroscopy, electron impact data, and the absorption and emission spectra of the nitromethane anion. Only the X and the A states are over determined from experimental data. Five curves in the C−H dimension have been calculated. All are in agreement with experimental data for the gas-phase acidity of nitromethane, the electron affinity of the CH_2NO_2 radical and the electron impact formation of the CH_2NO_2 anion. Curves for α-nitrotoluene have been predicted based on limited data, theoretical calculations, and by analogy to those of nitromethane.

Acknowledgment. We thank the Robert A. Welch Foundation, Grant E095, and UH−Clear Lake, Grant BC-0022, for support of this work. The important suggestions of the reviewer are greatly appreciated.

Nomenclature

α region = alpha region in the temperature dependence of the response of the electron capture detector; the slope in this region is proportional to the adiabatic electron affinity

A_{-1} = preexponential term for the rate constant for thermal electron attachment

A_1 = preexponential term for the rate constant for thermal electron detachment

A_2 = preexponential term for the rate constant for anion dissociation

A_D = pseudo-first-order recombination coefficient for electrons and positive ions

AEA = adiabatic electron affinity

AM1-MCCI = Austin model-1 multiconfiguration configuration interaction

A_N = pseudo-first-order recombination coefficient for negative and positive ions

β = exponential constant in the Morse potential

β region = the low-temperature region in the ECD data where A_1 and E_1 are determined

CH, CN = carbon−hydrogen bond distance, carbon−nitrogen bond distance

CURES EC = an acronym for the procedure used to minimize the deviation between the calculated and experimental electron affinities by adjusting the number of orbitals used in the configuration interaction

δ region = the high-temperature region in the ECD data where A_1 and E_1 are determined

D_e = dissociation energy referenced to the minimum in the pseudo two-dimensional potential energy curves

D(XY) = X−Y bond dissociation energy

DBEA= dipole bound electron affinity

DeBA = maximum value of A_1 determined from the de Broglie wavelength of the electron

E_{-1} = energy term for the rate constant for thermal electron attachment

E_1 = energy term for the rate constant for thermal electron detachment

E_2 = energy term for the rate constant for anion dissociation

EA = electron affinity = $-E_1 + E_{-1}$

ECD = electron capture detector

GPA = gas-phase acidity

K = electron capture detector molar response

k_A, k_B, k_R = dimensionless constant which modifies the Morse curves of the neutral to give the Morse curves for the anions

ν_e = frequency of the vibration in the pseudo two-dimensional Morse curves

PES = photoelectron spectroscopy

PFR = partition function ratio

r_e = internuclear distance in the pseudo two-dimensional Morse potential energy curves

READS TCT = acronym for a quantum mechanical simulation of electron transfer in the gas phase used to estimate relative electron affinities

RHF(*aann*) = restricted Hartree−Fock calculations with *aa* orbitals for configuration interaction in the negative ion and *nn* orbitals in the neutral

VEA = vertical electron affinity

References and Notes

(1) Steelhammer, J. C. M.S. Thesis, University of Houston, 1969.

(2) Freeman, R. R. Doctoral Dissertation, University of Houston, 1971.

(3) Chen, E. C. M.; Wentworth, W. E. *J. Phys. Chem.* **1983**, *87*, 45.

(4) Jager, K.; Henglein, A. *Z. Naturforsch.* **1967**, *22a*, 700.

(5) Stockdale, J. A.; Davis, F. J.; Compton, R. N.; Klots, C. E. *J. Chem. Phys.* **1974**, *60*, 4279.

(6) DeDomenico, A.; Franklin, J. L. *Int. J. Mass. Spectrom. Ion. Phys.* **1972**, *9*, 171.

(7) Compton, R. N.; Reinhardt, P. W.; Cooper, C. D. *J. Chem. Phys.* **1978**, *68*, 4360.

(8) Grimsrud, E.; Caldwell, G.; Kebarle, P. *J. Am. Chem. Soc.* **1985**, *107*, 4627.

(9) Lobo, R. F. M.; Moutinho, A. M. C.; Lachmann, K.; Los, J. *J. Chem. Phys.* **1991**, *95*, 166.

(10) Compton, R. N.; Carman, H. S.; Desfrancois, C.; Abdoul-Carmine, H. Schermann, J. P.; Hendricks, J. H.; Lyapustina, S. A.; Bowen, K. H. *J. Chem. Phys.* **1996**, *105*, 3475.

(11) Gutsev, G. L.; Bartlett, R. J. *J. Chem. Phys.* **1996**, *105*, 8785.

(12) Chen, E. C. M.; Wentworth, W. E. *Mol. Cryst. Liq. Cryst.* **1989**, *171*, 271.

(13) Christodoulides, C. C.; McCorkle, D. L.; Christophorou, L. G. in *Electron−Molecule Interactions and their Applications*; Academic Press: New York, 1984; Vol. 2, p 551.

(14) Lias, S. G.; Bartmess, J. E.; Liebman, J. F.; Holmes, J. L.; Levin, R. D.; Mallard, W. G. *J. Phys. Chem. Ref. Data* **1988**, Suppl. 1, 17.

(15) McMillen, D. F., Golden, D. M. *Annu. Rev. Phys. Chem.* **1982**, *33*, 493.

(16) Gruzdkov, Y. A.; Gupta, Y. M. *J. Phys. Chem. A* **1998**, *102*, 8325.

(17) Cummings, J. B.; Kebarle, P. *Can. J. Chem.* **1978**, *56*, 1.

(18) Bartmess, J. E.; Scott, J. A.; McIver, R. T. *J. Am. Chem. Soc.* **1979**, *101*, 6047.

(19) Metz, R. B.; Cyr, D. R.; Neumark, D. M. *J. Phys. Chem.* **1991**, *95*, 2900.

(20) Brinkman, E. A.; Gunther, E.; Schafer, O.; Brauman, J. I. *J. Chem. Phys.* **1994**, *100*, 1840.

(21) Wentworth, W. E.; Limero, T.; Batten, C. F.; D'sa, E. D.; Chen, E. C. M. *J. Chem. Phys.* **1988**, *88*, 4711.

(22) Chen, E. S. D.; Chen, E. C. M. *Chem. Phys. Lett.* **1998**, *293*, 491.

(23) Wiley, J. R.; Chen, E. C. M.; Wentworth, W. E. *J. Phys. Chem.* **1993**, *97*, 1256.

(24) Thoss, M.; Domcke, W. *J. Chem. Phys.* **1998**, *109*, 6577.

(25) Chen, E. C. M.; George, R.; Carr, S.; Wentworth, W. E.; Chen, E. S. D. *J. Chromatogr. A* **1998**, *811*, 250. Chen, E. C. M.; Carr, S.; Wentworth, W. E.; Chen, E. S. D. *J. Chromatogr. A* **1998**, *827*, 91.

(26) Chen, E. S. D.; Chen, E. C. M.; Sane, N. *Biochem. Biophys. Res. Commun.* **1998**, *246*, 228.

(27) Chen, E. S. D.; Chen, E. C. M.; Kozanecki, N. *J. Chem. Phys.* **1998**, *108*, 8749.

(28) Chen, E. S. D.; Chen, E. C. M.; Sane, N. *Bioelectrochem. Bioenerg.* **1998**, *46*, 15.

(29) Chen, E. S. D.; Chen, E. C. M.; Sane, N.; Schulze, S. *Bioelectrochem. Bioenerg.* **1999**, *48*, 69.

(30) Chen, E. C. M.; Wiley, J. R.; Batten, C. F.; Wentworth, W. E. *J. Phys. Chem.* **1994**, *98*, 88.

(31) Wentworth, W. E.; Chen, E. C. M.; Lovelock, J. E. *J. Phys. Chem.* **1966**, *70*, 445.

(32) Wiley, J. R.; Robinson, J. M.; Ehdaie, S.; Chen, E. C. M.; Chen, E. S. D.; Wentworth, W. E. *Biochem. Biophys. Res. Commun.* **1991**, *180*, 841.

(33) Aflatooni, K.; Gallup, G. A.; Burrow P. D. *J. Phys. Chem. A* **1998**, *102*, 6205.

(34) Hendricks, J. H.; Lyapustina, S. A.; deClerq, H. L.; Bowen, K. H. *J. Chem. Phys.* **1998**, *108*, 8.

(35) Huels, M. A.; Hahndorf, I.; Illenberger, E.; Sanche, L. *J. Chem. Phys.* **1998**, *108*, 1309.

(36) Brink, C.; Andersen, L. H.; Hvelplund, P.; Mahur, D.; Voldstad, J. D. *Chem. Phys. Lett.* **1998**, *233*, 52.

(37) Pack, J. L.; Phelps, A. V. *J. Chem. Phys.* **1966**, *45*, 4613.

(38) Taylor, H. S.; Goldstein, E.; Segal, G. A. *J. Chem. Phys.* **1977**, *10*, 2253.

(39) Wenthold, P. G.; Hrovat, D.; Borden, W. T.; Lineberger, W. C. *Science* **1996**, *272*, 1456.